SUPPLEMENTARY INFORMATION

SUPPLEMENTARY FIGURE 1

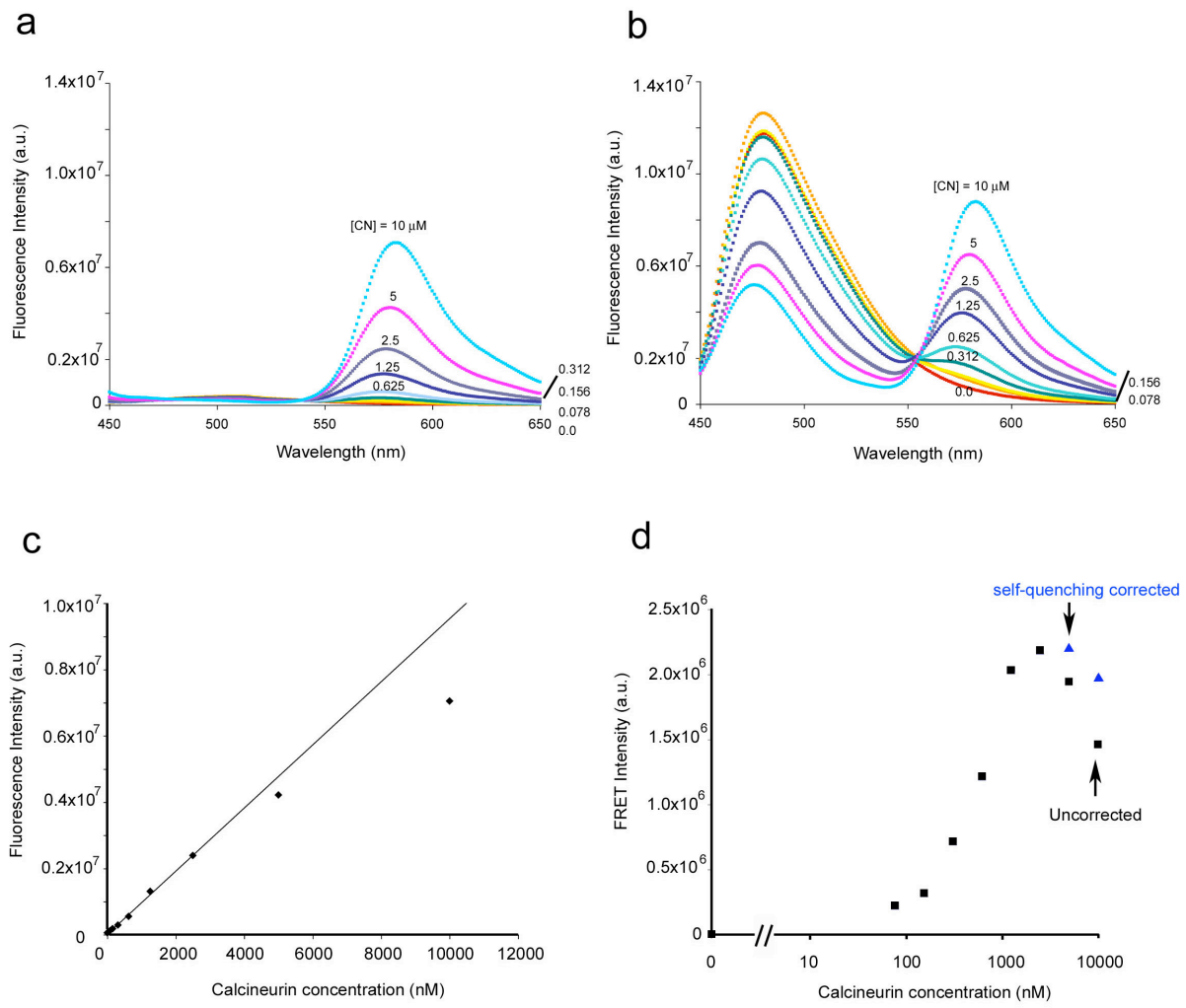

Supplementary Figure 1. FRET assay of CN-AKAP79 binding. (**a**) Fluorescence emission spectra of tetramethylrhodamine-CN (TMR-CN) alone at the indicated concentrations, with excitation at 436 nm. The increase in the emission peak with increasing CN is due to direct excitation of TMR acceptor at the donor excitation wavelength. (**b**) Fluorescence emission spectra of samples containing 100 nM ATTO 425-AKAP79 and the indicated concentrations of TMR-CN. The further increase of the acceptor peak at each concentration of CN and the quenching of the donor peak are diagnostic of energy transfer. (**c**) Emission at 582 nm of the CN samples in panel a is linear with CN concentration below 5 μM, then increases less steeply, consistent with self-quenching. (**d**) Fluorescence emission due to ATTO 425–TMR FRET in the experiment of panel b, after subtracting the components attributable to direct excitation of acceptor and to donor bleedthrough, plotted against log(CN concentration). For 5 μM and 10 μM CN, data points are plotted both without and with a correction for the self-quenching observed in panel c. The binding curve is comparable to that obtained independently in the stopped-flow experiments, Figures 3a and 3b, but the stopped-flow approach is more quantitatively reliable, because all corrections unrelated to the protein-protein binding interaction are subsumed in the zero time point.

SUPPLEMENTARY FIGURE 2

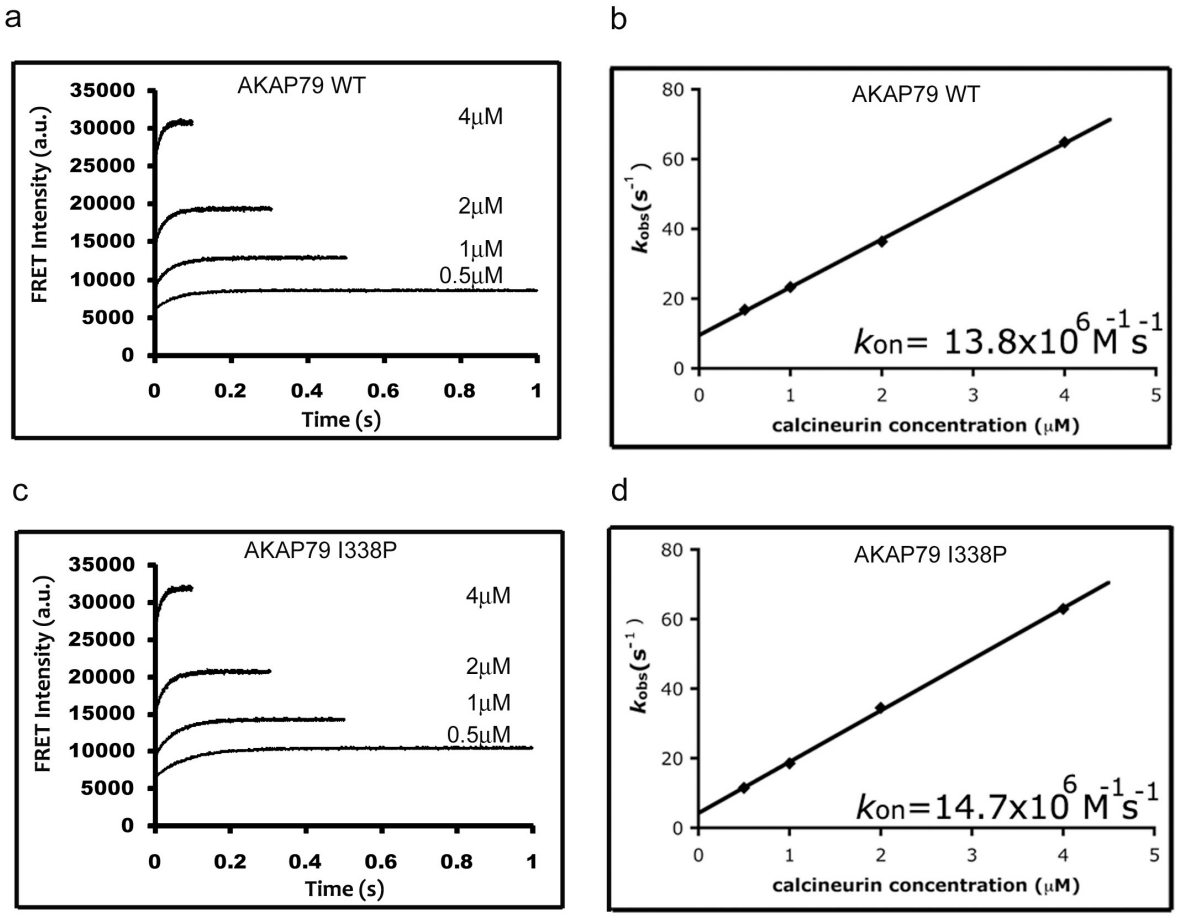

Supplementary Figure 2. CN-AKAP79 association kinetics at 36ºC. (**a**) Association of CN with wildtype AKAP79(333–408). (**b**) The association rate constant, k_{on}, for the CN–AKAP79 complex is determined by plotting the observed association rates, k_{obs}, against CN concentration. (**c**) Association of CN with the I338P variant of AKAP79(333–408). (**d**) Determination of the association rate constant, k_{on}, for CN binding to the I338P variant of AKAP79. The kinetic parameters translate to K_ds ~0.7 μM for wildtype and ~0.3 μM for I338P at physiological temperatures.

SUPPLEMENTARY FIGURE 3

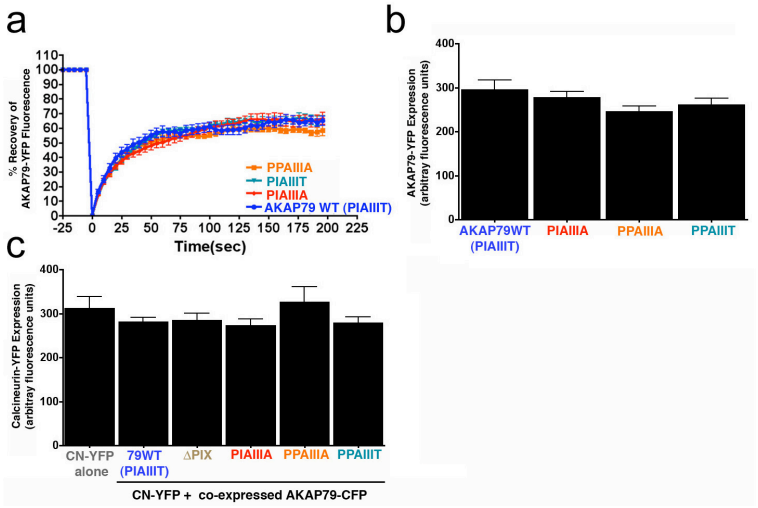

Supplementary Figure 3. Expression and mobility of AKAP79 proteins in cultured hippocampal neurons. (**a**) FRAP fluorescence recovery curves are similar for YFP-tagged wildtype AKAP79 and for YFP-tagged AKAP79 proteins with the indicated mutations in the CN-anchoring site. (**b**) Levels of expression of AKAP79-YFP WT and CN-anchoring site mutants in hippocampal neurons are similar. (**c**) Levels of expression of CN-YFP are similar when CN is expressed alone in hippocampal neurons or co-expressed with the indicated AKAP79 constructs. FRAP experiments were performed as described in Methods.

SUPPLEMENTARY METHODS

Protein expression and purification. Hexahistidine-tagged CNA was expressed together with CNB in *E. coli* strain BL21(DE3) from a tandem CNA-CNB expression construct in pET15b (ref. 1). The same modified CN expression construct was used as for crystallization of the CN–PVIVIT complex[2], with CNA truncated at residue 381, C-terminal to the CNB-binding helix, and CNB residues 2–15 omitted. Briefly, bacteria were grown at 37 ºC to OD_{600} 0.5, protein expression was induced at 18 ºC with 0.5 mM IPTG, and cells were harvested 48 hours later. CNA–CNB heterodimer was initially purified over a Ni^{2+}-NTA column (Qiagen), the hexahistidine tag was cleaved by overnight digestion with thrombin at 4 ºC, and the protein was again passed through a Ni^{2+}-NTA column to remove the cleaved peptide tag. CN was further purified on a phenyl sepharose column (Phenyl Sepharose High Performance, GE Healthcare) and an S200 size exclusion column (Superdex 200, Prep Grade, GE Healthcare).

cDNAs encoding human AKAP79 residues 333–408 and the docking and dimerization domain (D/D) of the RIIα regulatory subunit of PKA were cloned in tandem into the pT7SN/GpA vector (a gift from Don Engelman) after the staphylococcal nuclease (SN) coding sequence. A Shine-Delgarno sequence was incorporated before the coding sequence of RIIα, and residues 387–403 in the RIIα-anchoring portion of AKAP79 were replaced with the AKAP-*IS* sequence[3,4], which confers higher affinity for RIIα. Bacterial strain BL21(DE3) transformed with the AKAP79-RII construct was grown at 37 ºC to OD_{600} 0.6. Protein expression was induced with 0.5mM IPTG for 3 hours, and cells were lysed by probe sonication in buffer containing 50 mM Tris HCl, pH 7.5, 300 mM NaCl, 20 mM imidazole, 1 mM TCEP with 0.1 μg/mL aprotinin, 0.1 μg/mL leupeptin and 1 mM PMSF. The clarified lysate was passed through a Ni^{2+}-NTA column (Qiagen), and bound protein was eluted with an imidazole gradient from 50 mM to 350 mM. Fractions containing AKAP–RII complex were pooled, loaded onto an ion-exchange column (SP Sepharose high performance, GE Healthcare) pre-equilibrated with buffer containing 50 mM Tris HCl pH 7.5, 50 mM NaCl and 1 mM TCEP, and eluted with a NaCl gradient from 50 mM to 2 M. Concentrated AKAP–RII was subjected to size-exclusion chromatography using an S200 column (Superdex 200, Prep Grade, GE Healthcare). Finally, the SN moiety was cleaved by incubation with thrombin at 4 ºC and removed by passing the digestion mixture over a Ni^{2+}-NTA column. A stable calcineurin–AKAP79–RII complex was obtained by mixing purified CNA–CNB heterodimer and AKAP–RII complex at 1:1.5 ratio, followed by gel-filtration on an S200 column.

For binding studies using GST fusion proteins, cDNAs encoding wildtype and mutant AKAP79, residues 333–348 or 333–408 (again with the RII-binding site modified), were cloned into pGEX-2T vector, and the GST fusion proteins expressed in BL21(DE3) cells by overnight induction with 0.2 mM IPTG at 25 ºC. Bacterial pellets were lysed in PBS buffer with 1 mM PMSF, 0.1 μg/mL aprotinin, 0.1 μg/mL leupeptin, and 2 mM DTT by probe sonication on ice. The cleared lysate from 1 L culture was incubated with 1 mL bed volume of glutathione Sepharose (GE Healthcare) beads overnight. After ample washing with PBS buffer, GST fusion proteins were eluted by 20 mM reduced glutathione in PBS.

AKAP79 constructs for expression in hippocampal neurons. AKAP79 PIAIIIT-site mutant constructs were generated using Quikchange PCR. Reactions were performed using an annealing temperature ranging from 50–60ºC, elongation of 12 min at 68 ºC, and 18 cycles. PFU Turbo enzyme and buffer were used according to protocol (Stratagene, La Jolla, CA). Each reaction contained 5 ng DNA, 125 ng each forward and reverse primer, and 25 nM dNTP mixture. Following each successful reaction, cells were transformed and DNA was either mini- or maxi-prepped, and either used for sequencing or transfection into cells. Gene sequencing was performed by the University of Colorado Denver (UCD) sequencing core and sequence analysis was carried out using Macvector (Accelrys, San Diego, CA) to confirm mutations.

Crystallization and structure determination. Purified CN–AKAP79–RII complex, 10 mg/mL in 20 mM TES pH 7.0, 50 mM $CaCl_2$ and 1 mM DTT, was initially sent to Hauptman-Woodward Medical Research Institute for a high-throughput crystallization screening trial. Promising conditions from the screening trial were optimized to obtain high quality crystals using the sitting drop method at 20 ºC. The best crystals were grown when 7 mg/mL of the protein complex was mixed at 1:1 ratio with reservoir buffer containing 50 mM TES pH 7.5, 15% PEG 20,000, 100 mM $MgSO_4$, and 2 mM DTT at 20 ºC. Small plate-shaped crystals appeared overnight and continued to grow to about 0.4 x 0.15 x 0.05 mm^3 in a week. Crystals were flash-frozen in cryo-loops using reservoir buffer plus 30% MPD in liquid nitrogen. X-ray diffraction data were collected on NE-CAT beamline 24-ID-C at the Advanced Photon Source and processed with HKL-2000 software (HKL Research, Charlottesville, VA)[5]. Wavelength of data collection, 0.9789 Å; temperature, 105 K. The crystals belong to the $P2_12_12_1$ space group, with unit cell dimensions *a*=86.28 Å, *b*=89.70 Å, and *c*=158.91 Å. Diffraction data from one single crystal were used. The structure (PDB ID 3LL8) was solved by molecular replacement using the coordinates of a CNA–CNB complex from PDB entry 2P6B as a search model in Phaser[6], and was refined to 2.0 Å resolution using CNS[7]. The *R* factor and R_{free} for the final model are 18.0% and 22.8%, respectively. Ramachandran statistics: 96.8% favored, 0.2% outliers. Data collection and refinement statistics are listed in Table 1. There are two copies of the CNA/CNB heterodimer in the asymmetric unit, giving a solvent content of 52%. The final model contains CNA (residues 14 to 370 for both copies, molecules A and C) and CNB (residues 15 to 160 for molecule B, and residues 15 to 167 for molecule D). Though AKAP–RII formed a stable complex with CNA–CNB heterodimer, only residues 336–346 of AKAP79 were observed in the electron density map, and the RIIα D/D domain was not observed. Figures 1b, 1e, and 1fF were prepared using Chimera[8] and Figures 1c and 1d using Coot[9].

SEC-MALS. SEC-MALS experiments were performed on a light scattering system (Wyatt Technology Corporation, Santa Barbara, CA) comprising a DAWN EOS detector and an Optilab rEX refractive index detector coupled to an ÄKTA Purifier (GE Healthcare, Piscataway, NJ). Protein samples (5 mg/mL) of purified CN, CN–AKAP79 complex, or BSA were chromatographed on a Superdex 200 column. Data were analyzed using Astra V software (Wyatt Technology).

Calcineurin-AKAP79 competitive binding assays. The GST-AKAP79(333–408) fusion protein described above was used in competitive binding assays. GST-fusion constructs were used in the case of 14mer peptides, as well, because it proved difficult to obtain synthetic peptides of adequate purity due to suboptimal incorporation of successive isoleucines in the IAIIIT sequence. Concentrations of GST-protein and GST-peptide fusions were estimated using Bradford reagent (Bio-Rad, Medford, MA) and the use of comparable concentratoins confirmed by SDS-PAGE with the GST constructs at normalized concentrations (Figure 4a). The ability of the GST-AKAP79 constructs to compete with fluorescent PVIVIT peptide for binding to calcineurin was measured as described[10]. GST itself did not compete.

Measured anisotropies $\mathcal{A}$ were scaled to the corresponding fractional binding of fluorescent PVIVIT,

$$Y = \mathcal{F}_0 \, (\mathcal{A} - \mathcal{A}_{min}) \, / \, (\mathcal{A}_{max} - \mathcal{A}_{min}),$$

where Y is the scaled anisotropy; $\mathcal{F}_0$ is the fraction of fluorescent PVIVIT bound to CN in the absence of competitor, a solution of $[L \mathcal{F}_0^{\,2} - (K_d + L + R) \mathcal{F}_0 + R] = 0$ (refs. 11,12); and $\mathcal{A}_{max}$ and $\mathcal{A}_{min}$ were determined as described below. The scaled values were fitted to the equation

$$X Y (1 - Y) K_d = [(K_d Y + K_i (1 - Y)] [L Y^2 - (K_d + L + R) Y + R],$$

where X is total competitor concentration (free + bound), K_d is the known value for CN-fluorescent PVIVIT binding (0.5 μM), K_i refers to CN-competitor binding, L is total fluorescent PVIVIT concentration, and R is total CN concentration[11,12]. In all experiments, $\mathcal{A}_{max}$ was the average anisotropy in samples lacking competitor. For GST-peptide competition, $\mathcal{A}_{min}$ was the average anisotropy of free fluorescent PVIVIT peptide. Anisotropy values measured in the presence of GST-peptide competitor were corrected for the small increase in anisotropy seen both in samples of free fluorescent PVIVIT and in samples of CN–PVIVIT complex upon addition of GST. For GST-AKAP79 competition, $\mathcal{A}_{min}$ was the plateau reached at high competitor concentrations (PPAIIIT and PIAIIIT) or the anisotropy of free fluorescent PVIVIT in the cases where a plateau was not reached (PPAIIIA and PIAIIIA). Competitive displacement data are plotted against total competitor concentration in the assay.

FRET-based equilibrium binding and stopped-flow kinetic studies. For FRET measurements, we chose ATTO 425 dye (ATTO-TECH, Siegen, Germany) as donor and tetramethyl rhodamine (Invitrogen, Carlsbad, CA) as acceptor. For site-specific labeling of AKAP79(333–408) and its mutants, the pGEX-2T expression vector described above was modified to encode a Ser>Cys replacement at the P2' position of the pGEX-2T thrombin cleavage site, N-terminal to the AKAP79 fragment. The proteins were expressed and purified following the procedure described above, except that the last wash step was with 1X thrombin cleavage buffer, and the AKAP79 proteins were released from glutathione Sepharose beads by overnight cleavage with thrombin at 4 ºC. The proteins were concentrated to about 2 mg/mL using an Amicon Ultra centrifugal filter unit with 10 kDa molecular weight cutoff (Millipore, Billerica, MA). In the labeling reaction, ATTO 425-maleimide was

incubated with purified AKAP79 at 10:1 ratio overnight at 4 ºC. The reaction was stopped with excess DTT, and the mixture was passed through a PD-10 column (GE Healthcare, Piscataway, NJ) to remove free dye. Constructs encoding longer versions of AKAP-*IS* and its mutants, extending from residue 315 to residue 408, were also utilized for some experiments. In these cases a Ser321>Cys mutation was introduced for labeling.

For labeling of CN with acceptor fluorophore, we replaced Lys76 with Cys. Ala was substituted for the surface-exposed CNA residues Cys166, Cys184, Cys228, Cys256 and Cys336; and Val for Cys372. Cys154 in CNB was replaced by Val. This CN mutant was expressed and purified as described above. Tetramethylrhodamine maleimide was mixed with CN at 5:1 molar ratio and incubated at room temperature for 5 hours followed by removal of free dye using a PD-10 column.

Equilibrium FRET measurements were made on a HORIBA Jobin Yvon FLuoroLog-3 spectrofluorometer (Edison, NJ). Calcineurin (0.078 μM to 10 μM final concentration) was mixed with ATTO-labeled AKAP79 (100 nM final concentration). Fluorescence was excited at 436 nm, the absorption maximum for ATTO 425, and emission scans were taken from 450 nm to 650 nm. The FRET intensity was calculated by subtracting background, donor bleedthrough, and acceptor signal excited at the donor wavelength from the total measured fluorescence intensity. A correction for rhodamine self-quenching at concentrations of 5 μM or higher was made based on the quenching observed in solutions of CN alone (Supplementary Fig. 1).

FRET-based stopped-flow experiments were performed using a HI-TECH KinetAsyst stopped-flow system (model SF-61SX2; TgK Scientific, Bradford-on-Avon, UK) at two different temperatures, 22 ºC and 36 ºC. In association measurements, FRET transients were recorded at peptide concentration 100 nM and CN concentrations 0.5, 1, 2 and 4 μM. In dissociation measurements, a preformed complex of labeled AKAP79 peptide and calcineurin was mixed with excess unlabeled PVIVIT peptide to give final total concentrations 100 nM labeled AKAP, 2 μM CN, and 100 μM unlabeled PVIVIT in the dissociation reaction being monitored. Excitation was at 436 nm, and an OG590 cut-on filter was placed in the path of emitted light. Five transients were averaged for each data point. Single exponential curves were fitted to the association and dissociation data using GraphPad Prism (GraphPad Software, La Jolla, CA). An equilbrium binding curve was fitted to the FRET plateau data assuming reversible binding at a single class of sites.

FRET and YFP/CFP fluorescence ratio mesurements in MDCK cells. MDCK cells were plated on collagen-coated 25mm round glass coverslips in DMEM + 10% FBS media, grown for 48 h, and then transfected using Lipofectamine 2000 with cDNA plasmids (1–4 μg) encoding AKAP79-CFP and CNAα-YFP or PKA-RIIα-YFP, or linked CFP-YFP (provided by Alexander Sorkin, Univ. of Pittsburgh) at 50-60% confluency as previously described[13]. Living cells were imaged at room temperature 24–48 h post-transfection using a Nikon TE-300 inverted microscope equipped with a 63x or 100x plan-apo/1.4NA objective, Sensicam digital CCD camera, and Slidebook 4.0 software (Intelligent Imaging Innovations, Denver, CO). Three-filter FRET images were captured with 2x2 binning as described previously[13-15]. Briefly, YFP, CFP and CYFRET fluorescence were detected in single xy planes in

living cells using 250–500 ms exposure times to capture three images: 1) YFPexcitation/YFPemission, 2) CFP excitation/CFPemission, and 3) CFPexcitation/YFPemission (raw FRET). After background subtraction, fractional image subtraction corrected for CFP bleed-through and YFP cross-excitation,

FRETc = rawFRET – (0.5 * CFP) – (0.02 * YFP),

to yield an image of corrected FRET (FRETc), which was then gated to the CFP donor channel to create a FRETc/CFP pseudocolor image of relative FRET intensity in the cell.

Mean CFP, YFP, and raw FRET fluorescence intensities were measured by mask analysis of membrane regions (or the cytoplasm for linked CFP-YFP) in Slidebook 4.0 as described previously[14,15]. Apparent FRET efficiency (FRETeff) values were calculated from these mean intensities using the equation

FRETeff = FRETc / ((0.02 * YFP) * 10.6),

for a 1:1 complex, where FRETc is the emission from YFP due to FRET, 0.02 * YFP is the emission from YFP directly excited with the FRET filter cube, 10.6 is a factor relating CFP excited to YFP excited with the FRET filter cube, and (0.02 * YFP) * 10.6 is therefore the maximum sensitized YFP emission possible if every excited CFP transferred its excitation to the associated YFP[15-17]. In calculations for a 2:1 acceptor-donor complex, the denominator was halved, since an individual excited CFP could transfer its excitation to only one of the associated YFP acceptors. Average mean intensity levels for AKAP79-CFP (40–130 arbitrary fluorescence units (afu)), CNA-YFP (700–1200 afu), and PKA-RII-YFP (1400–1700 afu) expression were comparable across experimental conditions. Mean intensity values for CFP-YFP were also in the same range (CFP: 40–130 afu; YFP: 400–1200 afu). YFP/CFP fluorescence intensity ratios were corrected for CFP quenching due to FRET using the equation

YFP/CFPcorr = YFP / (CFP / (1 – FRETeff)).

Corrected YFP/CFP ratios for CN–AKAP pairs treated as 1:1 complexes (6.6±0.5 for wildtype AKAP79, 8.1±0.6 for the PPAIIIT variant) or treated as 2:1 complexes (6.1±0.4 for wildtype AKAP79, 7.1±0.5 for the PPAIIIT variant) differed only minimally, and did not exceed the ratio for the 1:1 CFP-YFP construct. Thus, in Figures 2g and 2h, only FRETeff values and corrected YFP/CFP ratios for a 1:1 CN–AKAP79 complex are plotted. The YFP/CFP ratio calculated for the RII–AKAP pair (25.2±1.2) is more than 2-fold greater than the ratio calculated for the 1:1 CFP-YFP construct (8.5±1.0). There is likely to be some amount of unanchored RII-YFP fluorescence contaminating our membrane measurements, which would artificially increase the denominator in the calculation of FRETeff and the numerator YFP in the calculation of YFP/CFP, thus rendering our calculation of a corrected YFP/CFP ratio for the RII-AKAP pair an overestimate. If 25–30% of RII-YFP in the region

analyzed is not associated with AKAP79-CFP, that would account for the deviation of the YFP/CFP ratio from the value expected for a 2:1 complex.

Primary culture and transfection of rat hippocampal neurons. Neurons were cultured as described previously[18]. Briefly, the hippocampus was dissected from P0-2 Sprague Dawley rats and dissociated with papain. Neurons were plated at medium density (200,000–300,000 cells/ml) on poly-D-lysine and laminin coated 12 mm glass coverslips or 35 mm glass bottom plates. Neurons were fed every 3 days *in vitro* (DIV) with Neurobasal-A (NB) medium plus B-27 and mitotic inhibitors (Invitrogen). For lipofectamine 2000 transfection (Invitrogen), DIV7-8 (NFAT translocation assays), DIV10-11 (live-cell FRAP imaging), or DIV12 (3xNFAT-AP1–CFP-NLS reporter assays) neurons were transfected; 250 µL NB + 10 µL of lipofectamine were combined in one tube and 250 µL NB + 2–4 µg total plasmids encoding cDNA/shRNAi were combined in a second tube and allowed to incubate at room temperature for 5 min. The pSil-ShRNAi AKAP150 vector used to knock down endogenous AKAP150 and allow rescue replacement with human AKAP79 has been previously described and show by us to effectively knock down AKAP150 expression in hippocampal neurons for 2–12 days post transfection[15,19,20]. The lipofectamine and DNA tubes were combined and allowed to incubate at room temperature for 20 min. During the 20-min incubation time, half of the medium was removed from the cultured cells and mixed equally with fresh NB (+B-27, mitotic inhibitors) and saved. Following the 20-min incubation, 500µL of the lipofectamine+DNA mixture was added to the cultured neurons and allowed to incubate for 2 h at 37ºC, 5% CO_2. Subsequently, the medium was replaced with the culture medium that had been saved. The neurons were then incubated at 37ºC, 5% CO_2, and used within 2 days for live-cell FRAP imaging at DIV 12-13 or incubated for 5-6 days and then treated with the KCl stimulation protocol and fixed for NFAT immunostaining at DIV 12-14 (see below).

NFAT translocation assays in hippocampal neurons. DIV12-14 cultured hippocampal neurons (5–6 days post-transfection) were placed in a Tyrode's salt solution including 1µM TTX (Tocris) to dampen spontaneous activity and lower basal levels of NFAT nuclear translocation[15]. Cells were incubated in Tyrode's + TTX at 37ºC, 5% CO_2, for 3 h. Subsequently, cells were placed in a perfusion system and control Tyrode's solution without TTX was perfused across the cells for 5 min, followed by a 3-min perfusion with an isotonic 90 mM KCl Tyrode's solution to depolarize the cells and activate the L-type Ca^{2+} channels. Next, cells were perfused for 5 min with control Tyrode's solution to remove residual KCl and allowed to recover for 5, 15, 60 and 90 min in control Tyrode's solution containing 1 µM TTX at 37ºC, 5% CO_2. Cells then underwent immunocytochemistry to stain endogenous NFAT3 (also termed NFATc4) essentially as described[18]. Briefly, after treatments, cultured hippocampal neurons were fixed for 10 min at room temperature with 3.7% paraformaldehyde in PBS, followed by permeabilization for 10 min at room temperature in 0.2% TritonX-100 in PBS. Next, cells were blocked in 10% BSA/PBS overnight at 4ºC. Primary antibodies (NFAT3/c4; Santa Cruz) were diluted 1:100 in 10% BSA/PBS and incubated for 2 hrs at room temperature. After incubation with primary antibody, cells were washed twice in PBS, followed by a single wash in 10% BSA/PBS. Cells were then incubated in Texas Red secondary antibody (goat anti-mouse; Invitrogen), diluted 1:500, for 1.5

h at room temperature. Coverslips containing cells were then washed twice in PBS and once in Milli-Q water before mounting on glass slides with Pro-long gold (Invitrogen) containing DAPI.

NFAT transcriptional reporter assays in hippocampal neurons. The 3xNFAT-AP1–CFP-NLS reporter construct was generated from a 3xNFAT-AP1–luciferase reporter construct[21] by replacing a BglII–EcoRV fragment immediately downstream of the HSV tk promoter with a cDNA encoding CFP-NLS. The inserted BglII–EcoRV fragment was an ~800 bp synthetic DNA consisting of a Kozak sequence, the cDNA for ECFP fused in frame to three copies of cDNA encoding the SV40 nuclear localization sequence (NLS), and stop codons in all three reading frames. Hippocampal cultures grown on 12-mm glass coverslips for 12 DIV were transfected using Lipofectamine 2000 with the 3xNFAT-AP1–CFP-NLS reporter plasmid and other cDNA or shRNAi plasmids as described above. 4 h or 26 h after transfection (for 16 h or 6 h post-KCl conditions, respectively, to ensure in both cases that cDNA and RNAi constructs would be expressed for a total of ~2 days post-transfection before fixation) 1μM TTX was added in conditioned NB culture medium for 24 h at 37ºC, 5% CO_2, to dampen spontaneous activity and decrease basal CFP expression. After this TTX pretreatment, neurons were subjected to a 5 min wash in control Tyrode's followed by a 3 min depolarization with isotonic 90 mM KCl as above. Residual KCl was removed with an additional 5 min control Tyrode's wash and cells were returned to conditioned NB media containing 1μM TTX for 6 or 16 h at 37ºC, 5% CO_2. Hippocampal neurons were fixed in 3.7% formaldehyde in PBS, permeabilized with 0.05% Triton X-100 in PBS, stained with a 1 μM solution of propidium iodide (PI) to visualize the nucleus, and mounted onto glass slides as above.

Hippocampal neuron fluorescence microscopy. A Zeiss Axiovert 200M microcope with either 100x or 63x plan-apo/1.4NA objective, 150–300 W xenon illumination, Coolsnap CCD camera, and Slidebook 4.2–5.0 software (Intelligent Imaging Innovations, Denver, CO) was used for live-cell YFP FRAP and fixed-cell fluorescence imaging of NFAT3, DAPI or PI (images not shown), CFP and YFP. For FRAP, neurons were maintained at 32ºC, 5% CO_2, and single xy-plane images were taken. Time-lapse FRAP images were used for quantitative analysis of mean fluorescence intensity changes over time as described in more detail below. Fixed cells were imaged by acquiring 5 μm 3D z-stacks of xy planes with 0.5 μm steps centered on the neuronal cell body. Images were deconvolved to nearest neighbors to generate confocal sections that were then collapsed into 2D sum intensity projection images and used for quantitative mask analysis in Slidebook 4.2–5.0 to measure mean NFAT nucleus/cytoplasm immunofluorescence intensity ratios[15] or mean CFP fluorescence intensity in the nucleus. Briefly, by restricting the 3D z-stack to 5 μm centered on the nucleus, the contribution of superior and inferior perinuclear cytoplasmic NFAT3 staining was excluded from the measurement of nuclear NFAT in the sum intensity projection image. Masks for the nucleus were created by tracing the entirety of the DAPI stained nucleus. Masks for the cytoplasm were created by omitting the stained nucleus during tracing of the neuronal soma. For the CFP-NLS transcriptional reporter experiments, PI staining was used to define the mask for the nucleus. Mean fluorescence intensities were then extracted from the nucleus and cytoplasm masks to determine NFAT nucleus-to-cytoplasm ratios or mean CFP intensity expressed in the nucleus. Statistical comparisons of nucleus/cytoplasm

ratios or mean CFP fluorescence in the nucleus across groups were carried out using GraphPad Prism 4.0 by one-way ANOVA with Bonferroni's post-hoc analysis or student's t-test.

FRAP microscopy. A micro-point tunable laser ablation system (Photonic Instruments, St Charles, IL) focused through the epi-fluorescence optics of the Zeiss Axiovert 200M was used to photobleach a single dendritic spine in cultured dissociated rat hippocampal pyramidal neurons. After the capture of five pre-bleach baseline images at 5 s intervals, 515 nm laser pulses were directed at single dendritic spines for 2 repetitions at 75-85% maximum laser power to bleach YFP selectively. Directly after bleaching, 40 time-lapse images were captured at 5 s intervals. Pre-bleached intensities were averaged and set to 100% and the immediate post-bleach image was set to 0% (refs. [22,23]). This allowed for the combination of data from different experiments within groups and the comparison of data across groups. Pooled recovery curves were fit using a one-phase exponential association non-linear regression in GraphPad Prism 4.0. These fits gave maximal % recovery (mobile pool size) values[22,23]. Subsequent statistical comparisons were made by one-way ANOVA with Bonferroni's post-hoc analysis.

REFERENCES

1. Mondragon, A. *et al*. Overexpression and purification of human calcineurin α from *Escherichia coli* and assessment of catalytic functions of residues surrounding the binuclear metal center. *Biochemistry* **36**, 4934-4942 (1997).
2. Li, H., Zhang, L., Rao, A., Harrison, S.C. & Hogan, P.G. Structure of calcineurin in complex with PVIVIT peptide: portrait of a low-affinity signalling interaction. *J. Mol. Biol.* **369**, 1296-1306 (2007).
3. Alto, N.M. *et al*. Bioinformatic design of A-kinase anchoring protein-*in silico*: A potent and selective peptide antagonist of type II protein kinase A anchoring. *Proc. Natl. Acad. Sci. USA* **100**, 4445-4450 (2003).
4. Gold, M.G. *et al*. Molecular basis of AKAP specificity for PKA regulatory subunits. *Mol. Cell* **24**, 383-395 (2006).
5. Otwinowski, Z. & Minor, W. Processing of X-ray diffraction data collected in oscillation mode. *Methods in Enzymology* **276**, 307-326 (1997).
6. McCoy, A.J. *et al*. Phaser crystallographic software. *J. Appl. Cryst.* **40**, 658-674 (2007).
7. Brunger, A.T. *et al*. Crystallography & NMR system: A new software system for macromolecular structure determination. *Acta Cryst.* **D54**, 905-921 (1998).
8. Pettersen, E.F. *et al*. UCSF Chimera— A visualization system for exploratory research and analysis. *J. Comput. Chem.* **13**, 1605-1612 (2004).
9. Emsley, P. & Cowtan, K. Coot: model-building tools for molecular graphics. *Acta Cryst D* **60**, 2126-2132 (2004).
10. Li, H., Rao, A. & Hogan, P.G. Structural delineation of the calcineurin-NFAT interaction and its parallels to PP1 targeting interactions. *J. Mol. Biol.* **342**, 1659-1674 (2004).
11. Wang, Z.X. An exact mathematical expression for describing competitive binding of two different ligands to a protein molecule. *FEBS Lett.* **360**, 111-114 (1995).
12. Roehrl, M.H. *et al*. Selective inhibition of calcineurin-NFAT signaling by blocking protein-protein interaction with small organic molecules. *Proc. Natl. Acad. Sci. USA* **101**, 7554-7559 (2004).

13. Gorski, J.A., Gomez, L.L., Scott, J.D. & Dell'Acqua, M.L. Association of an A-kinase-anchoring protein signaling scaffold with cadherin adhesion molecules in neurons and epithelial cells. *Mol. Biol. Cell* **16**, 3574-3590 (2005).
14. Oliveria, S.F., Gomez, L.L. & Dell'Acqua, M.L. Imaging kinase–AKAP79–phosphatase scaffold complexes at the plasma membrane in living cells using FRET microscopy. *J. Cell Biol.* **160**, 101-112 (2003).
15. Oliveria, S.F., Dell'Acqua, M.L. & Sather, W.A. AKAP79/150 anchoring of calcineurin controls neuronal L-type Ca^{2+} channel activity and nuclear signaling. *Neuron* **55**, 261-275 (2007).
16. Erickson, M.G., Alseikhan, B.A., Peterson, B.Z. & Yue, D.T. Preassociation of calmodulin with voltage-gated Ca^{2+} channels revealed by FRET in single living cells. *Neuron* **31**, 973-385 (2001).
17. Erickson, M.G., Liang, H., Mori, M.X. & Yue, D.T. FRET two-hybrid mapping reveals function and location of L-type Ca^{2+} channel CaM preassociation. *Neuron* **39**, 97-107 (2003).
18. Gomez, L.L., Alam, S., Smith, K.E., Horne, E. & Dell'Acqua, M.L. Regulation of A-kinase anchoring protein 79/150–cAMP-dependent protein kinase postsynaptic targeting by NMDA receptor activation of calcineurin and remodeling of dendritic actin. *J. Neurosci.* **22**, 7027-7044 (2002).
19. Hoshi, N., Langeberg, L.K. & Scott, J.D. Distinct enzyme combinations in AKAP signalling complexes permit functional diversity. *Nat. Cell Biol.* **7**, 1066-1073 (2005).
20. Robertson, H.R., Gibson, E.S., Benke, T.A. & Dell'Acqua, M.L. Regulation of postsynaptic structure and function by an A-kinase anchoring protein–membrane-associated guanylate kinase scaffolding complex. *J. Neurosci.* **29**, 7929-7943 (2009).
21. Hedin, K.E. *et al*. Delta-opioid receptors expressed by Jurkat T cells enhance IL-2 secretion by increasing AP-1 complexes and activity of the NF-AT/AP-1-binding promoter element. *J. Immunol.* **159**, 5431-5440 (1997).
22. Lippincott-Schwartz, J., Snapp, E. & Kenworthy, A. Studying protein dynamics in living cells. *Nat. Rev. Mol. Cell Biol.* **2**, 444-456 (2001).
23. Sharma, K., Fong, D.K. & Craig, A.M. Postsynaptic protein mobility in dendritic spines: long-term regulation by synaptic NMDA receptor activation. *Mol. Cell. Neurosci.* **31**, 702-712 (2006).